Transient Electromagnetic Fields Calculation around Transmission Lines using FDTD

Samy M. Ghania

University of Jeddah, Saudi Arabia

sghania@uj.edu.sa

ABSTRACT

For proper design of transmission and distribution insulation systems, it is necessary to fully clarify the characteristics of lightning phenomena. In this study, two typical power transmission lines, 500 and 220 kV, were modeled to compute the lightning electromagnetic fields around the transmission lines. The lightning electromagnetic fields around the different power lines were calculated using the Finite Difference Time Domain (FDTD) method with Maxwell's equations. Two selected zones were used to capture electromagnetic fields during lightning strikes. The first zone was around the insulators and the second was at the ground level below the power line at 1 m above ground and the power line Right Of Way (ROW). The correlation between the induced magnetic and electric fields was verified in the free space inside the two selected zones. The induced electromagnetic fields were evaluated at different positions of each power line phase. The results obtained showed that while lightning strikes the conductor, the waveforms of the electromagnetic field obtained at the selected monitoring points were the same as the waveform of the lightning current. The amplitude of the electromagnetic field intensities exhibited a stable linear relationship with the lightning currents as the intrinsic impedance of the free air. This study was mainly concerned with transient electromagnetic fields that could appear inside high-voltage substations to clarify the electromagnetic exposure levels around high-voltage transmission lines.

Keywords-transient electromagnetic fields; FDTD; transmission lines

I. INTRODUCTION

Characteristics of electric and magnetic fields produced by lightning discharges are the core of recent studies worldwide, as the lightning phenomenon is still full of mystery parameters that should be adequately addressed [1]. Lightning strikes to overhead power transmission lines are the main accidental reason for service outages or insulation damage. Recently, lightning strikes have produced overimposed electromagnetic waves on overhead power transmission lines. Subsequently, these electromagnetic waves have probable potential and direct influences on the insulation level design process [2-3]. The effects of the striking object presence on the radiated electric and magnetic fields are essentially dependent on its height and shape as well as on the distance from the observation points [4-6]. The lightning current waveform is a microsecond-scale waveform that is probably formed in the shape of downward negative lightning. Meanwhile, it is of the order of millisecond-scale waveform for subsequent strokes [7]. In the absence of a structure with a high height, most of the positive lightning is initiated by a positively charged downward leader. The highest directly measured current for positive lightning with a charge transfer of 100C is approximately 320 kA [8]. The measured current parameters of the positive and negative first strokes are considered in common weighted statistics. The damages caused by lightning are not significantly dependent on the direction of the current flow [9-10].

Lightning strikes have been observed for about three decades over the Canadian National Tower to simultaneously capture the lightning parameters and return-stroke current derivative at about 475 m above ground, using a Rogowski coil and broadband active sensors. In [11], a good linear correlation between the magnetic field wave and the current was detected. For modeling electromagnetic return-stroke, Maxwell's equations are solved to yield the distribution of current along the lightning channel using numerical techniques, such as the Method Of Moments (MOM) or the finite-difference method [12-15]. These approaches are the Cooray formula, exact evaluation of the field equation numerically, and numerical solution of Maxwell's equation using Finite Difference Time Domain (FDTD). The exact numerical solution and the FDTD are virtually identical. It has also been shown that the Cooray formula has good accuracy for underground fields, especially for their early time response. This study investigated the 3-D FDTD for solving Maxwell's equations to calculate lightning magnetic and electric fields around two typical 500 and 220 kV overhead transmission lines. Moreover, the field equation was solved with an exact solution analytically to verify the convergence of the two methods. To represent lightning electromagnetic fields, many Matlab M-Script files were developed based on three-dimensional field calculation techniques using FDTD. Electromagnetic fields were calculated at different points around the simulated towers and at the Right Of Way (ROW) of each line. The lightning current

was simulated based on the sum of the two Heidler's functions and its derivative to evaluate its suitability to simulate the lightning return-stroke current. The lightning magnetic and electric fields at the selected points around the towers were calculated. The simulation was developed using MATLAB M-scripts files, and the resulting 3D figures were developed using Mesh-3D.

II. TRANSMISSION LINES AND LIGHTNING CURRENT SIMULATION

A. System Configuration

Two power lines of 500 and 220 kV were simulated to calculate the lightning electromagnetic fields. The power line conductors of each phase were simulated as a series of connected current segments to closely fit the geometry of the catenary shape based on the Biot-Savart low in three dimensions and using FDTD [16-17]. Two different positions were selected to calculate the lightning electromagnetic fields at 1, 4, and 7 m from the ground and at 1 m from the power line conductors. Moreover, the electromagnetic fields were calculated over the entire area underneath the power line along two different directions, lateral and longitudinal. Figure 1 shows the main configurations of the two simulated lines. Lightning was assumed to strike the power line conductors of each line and the ground conductors to demonstrate their effects.
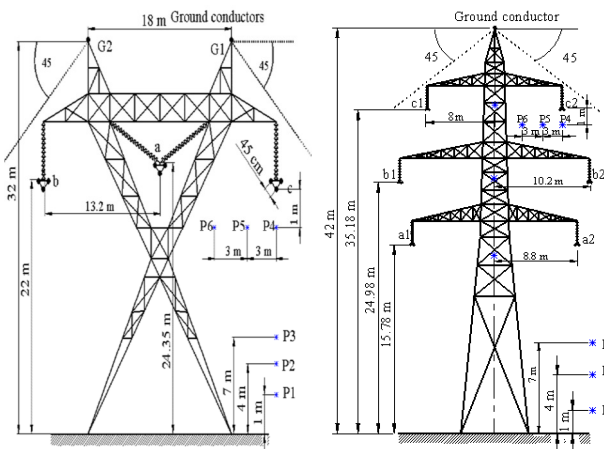

Fig. 1.   Modeled 500 kV and 220 kV towers with ground conductors.

B. Lightning Current Simulation

For the developed charges, cloud to ground or ground to cloud with different polarities, there are four different lightning strikes, depending on the cloud polarity to the ground, "positive or negative cloud" to "negative or positive" ground. Recent studies on lightning current simulation for the first and subsequent return strokes tackled the more appropriate analytical expression of the sum of the so-called Heidler's functions [18-19].

$$i(0,t) =$$
$$\left(\frac{I_{01}}{\eta_1}\left(\frac{\left(\frac{t}{\tau_{11}}\right)^n}{1+\left(\frac{t}{\tau_{11}}\right)^n}\right)exp\left(-\frac{t}{\tau_{12}}\right)\right) \quad +$$
$$\left(\frac{I_{02}}{\eta_2}\left(\frac{\left(\frac{t}{\tau_{21}}\right)^n}{1+\left(\frac{t}{\tau_{21}}\right)^n}\right)exp\left(-\frac{t}{\tau_{22}}\right)\right) \tag{1}$$

$$\eta = \exp\left[-\left(\frac{\tau_{i1}}{\tau_{i2}}\right)\left(n\left(\frac{\tau_{i2}}{\tau_{i1}}\right)\right)^{\frac{1}{n}}\right] \tag{2}$$

where I_{01} is the amplitude parameter of the front current, I_{02} is the amplitude parameter of the decay current, t_{i1} is the front time constant ($i = 1, 2$), τ_{i2} is the decay time constant ($i = 1, 2$), η is the amplitude correction factor, and n is the exponent (2,…,10). Assuming the highest protection level [20], Table I gives the parameters of the simulated double-exponential lightning currents.

TABLE I.   MAIN PARAMETERS OF THE SIMULATED LIGHTNING CURRENTS

Simulated stroke	Il (kA)	tf (μS)	tt (μS)	τ_1 (μS)	τ_2 (μS)	η
Positive first	200	10	350	470.1	4064	0.951
Negative first	100	1	200	284.3	373.9	0.990
Negative subs.	50	0.25	100	143.1	92.4	0.995

III. LIGHTNING ELECTROMAGNETIC FIELDS CALCULATION

A. Using Exact Field Equations (analytically)

Two simultaneous steps must be taken to evaluate the lightning electromagnetic fields. The first step is to calculate the currents on the conductors due to lightning. The second step is to calculate the radiated electromagnetic fields around the conductors due to the traveling current waveform. The lightning transient electromagnetic fields can be evaluated numerically or analytically by assuming the line or conductor to be a cylinder with a very small radius for the wavelength [21]. This is because the effective reflection is usually proportional to the target electrical size coupled with the frequency. Frequency should be in a microwave range greater than 100 MHz to be considered an effective reflection. Figure 2 shows a line segment of length L along the z direction from the origin and $P(x, y, z)$ is an arbitrary point in space around the conductor [22]. The electromagnetic field potential vector $\vec{A}_z(t)$ for a filament along the z-axis is presented while the X and Y components of the potential vector can be neglected [17]. The z component $A_z(t)$ created by current $i(\xi, t)$ flowing in the line at the point P can be expressed as:

$$A_z(t) = \frac{\mu_o}{4\pi}\int_0^L i(\xi, t - R(\xi)/c)/R(\xi)d\xi \tag{3}$$

$$i(\xi, t - \frac{R(\xi)}{c}) = i_g(t - \frac{\xi+R(\xi)}{c}) + i_f(t - \frac{-\xi+R(\xi)}{c}) \tag{4}$$

where ξ is the arbitrary point on the conductors, c is the speed of the light in free space (3×10^8 m/s), i_g is the current wave traveling in the forward direction, and i_f is the current wave traveling in the backward direction.
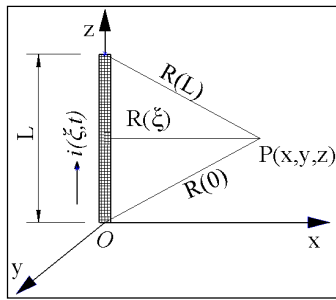
Fig. 2.   Simple presentation of the current segment.

The magnetic field can be evaluated by:

$$H_x(t) = \frac{1}{\mu_\circ} \frac{\partial A_z(t)}{\partial y}; \quad H_y(t) = -\frac{1}{\mu_\circ} \frac{\partial A_z(t)}{\partial x}; \quad H_z(t) = 0 \quad (5)$$

After determining the transient magnetic field, the transient electric field $\vec{E}(t)$ is calculated by integrating the curl of $\vec{H}(t)$ to get the three components of the electric field as follows:

$$E_x(t) = \frac{1}{\varepsilon_\circ} \int_0^t \frac{\partial H_y(t)}{\partial z} dt$$

$$E_y(t) = \frac{1}{\varepsilon_\circ} \int_0^t \frac{\partial H_x(t)}{\partial z} dt$$

$$E_z(t) = \frac{1}{\varepsilon_\circ} \int_0^t \left[\frac{\partial H_y(t)}{\partial x} - \frac{\partial H_x(t)}{\partial y} \right] dt \quad (6)$$

B. Using the FDTD Method

Maxwell's equations for driving sources and lossy dielectric materials are presented in (7) and (8). Expanding these two main equations over the Yee cell in space with the time domain [22-24] yields the main relations of electromagnetic fields in both the space and the time domains.

$$\frac{\partial \vec{H}}{\partial t} = -\frac{1}{\mu} \nabla X \vec{E} - \frac{\sigma}{\mu} \vec{H} \quad (7)$$

$$\frac{\partial \vec{E}}{\partial t} + \frac{\sigma}{\varepsilon} \vec{E} = \frac{1}{\varepsilon} \nabla X \vec{H} \quad (8)$$

Expanding *E* and *H* over the Yee cell in the space and time domains yields six subequations. These six equations present the main standard form of the FDTD algorithm used to monitor and capture the effects of the distribution of both magnetic and electric fields and their duality effects.

IV.   LIGHTNING ELECTROMAGNETIC FIELD RESULTS

A. For Normal Conditions

Table II shows the maximum lightning electromagnetic fields at different points below 500 and 220 kV, with the configurations shown in Figure 1, for normal operation with each power line loaded with 1 kA. The calculation is performed analytically and numerically to validate the accuracy of the FDTD algorithm. The percentage error was found to be less than 1% for 500 kV and less than 2% for 220 kV power lines. The maximum induced magnetic and electric fields were approximately 222 A/m and 83 kV/m at point No. 4 in the 500 kV power line under normal operation. The maximum induced magnetic and electric field values were approximately 191 A/m and 72 kV/m at point No. 4 in the 220 kV power line under

normal operation. Figure 3 presents the electromagnetic field profiles of 220 kV power lines for normal operation at 1 m above ground through an area between the mid-span of two subsequent line spans of one complete span with the tower positioned in the center of the electromagnetic field profiles. For the 500 kV power line, the maximum magnetic and electric field values were approximately 17 A/m and 10 kV/m at the mid-span position. Meanwhile, for the 220 kV power line, the maximum magnetic and electric field values were approximately 23 A/m and 13 kV/m at the mid-span position.

TABLE II.   MAXIMUM INDUCED ELECTROMAGNETIC FIELD FOR NORMAL OPERATION OF 500 AND 220 KV LINES

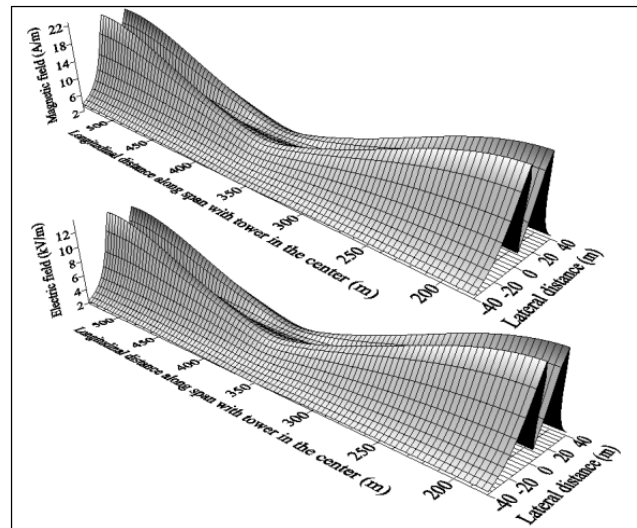| 500 kV	Magnetic field (A/m)			Electric field (kV/m)		
	Analyti-cally	Numeri-cally	% error	Analyti-cally	Numeri-cally	% error
P1	7.216	7.232	0.22	2.72	2.73	0.37
P2	8.968	8.992	0.27	3.37	3.39	0.59
P3	11.45	11.48	0.21	4.31	4.33	0.46
P4	222.4	222.8	0.18	83.91	83.97	0.072
P5	77.12	77.52	0.52	29.18	29.21	0.1
P6	51.76	51.79	0.05	19.49	19.52	0.15
220 kV	Magnetic field (A/m)			Electric field (kV/m)		
	Analyti-cally	Numeri-cally	% error	Analyti-cally	Numeri-cally	% error
P1	11.92	12.08	1.32	4.51	4.54	0.66
P2	13.86	13.87	0.12	5.21	5.23	0.38
P3	16.89	16.93	0.24	6.34	6.38	0.63
P4	191.4	191.5	0.09	72.1	72.18	0.11
P5	64.72	64.89	0.27	24.36	24.45	0.37
P6	40.67	40.69	0.06	15.31	15.34	0.20

Fig. 3.   Magnetic and electric field profiles around the 220 kV power transmission lines under normal conditions.

B. For Lightning Conditions

It was assumed that lightning strikes phase C of a 500 kV power line and phase C (circuit C2) of a 220 kV power line with a peak lightning current of 100 kA. Table III shows the maximum induced electromagnetic field values at the monitoring points under 500 and 220 kV. For 500 kV, the

maximum induced magnetic and electric field values were approximately 22.4 kA/m and 8.45 MV/m at the closest point to the striking point (P4). For 220 kV, the maximum induced magnetic and electric field values were approximately 22 kA/m and 8.3 MV/m at the closest point to the striking point (P4). Figure 4 illustrates the time-varying lightning electromagnetic field in the 500 kV power line at 1 m above ground during lightning strikes. Electromagnetic field profiles are presented along the lateral direction (x-direction) with a simulation time of 500 µs. The lightning electromagnetic fields have profiles similar to the waveforms of the lightning currents. Figure 4 also shows the electromagnetic field profiles at 1 m above ground for 500 µs with a peak striking current of 100 kA for the 500 kV power line. For 500 kV electromagnetic field profiles, the maximum induced magnetic and electric field values were approximately 1 kA/m and 376 kV/m. For 220 kV, the maximum induced magnetic and electric field values were approximately 615 A/m and 230 kV/m, respectively. A capture zone was selected to monitor the electromagnetic field profiles around the insulator surfaces during lightning. This zone was extended along an area of 10-16 m laterally and 18-26 m vertically for 500 kV. For 220 kV, the selected zone was extended along an area of 6-10 m laterally and 33-37 m vertically.

TABLE III.   MAXIMUM ELECTROMAGNETIC FIELD VALUES UNDER LIGHTNING FOR 500 AND 220 KV POWER LINES

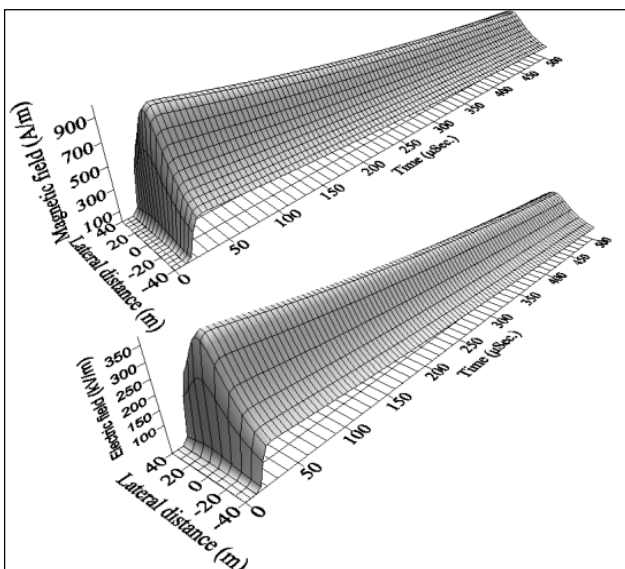|	Points	P1	P2	P3	P4	P5	P6
500 kV	(A/m)	1026	1201	1446	22430	6498	3338
	(kV/m)	386	452	544	8451	2448	1257
220 kV	(A/m)	612	664	735	22027	6499	3334
	(kV/m)	227	250	277	8299	2449	1256

Fig. 4.   Lightning electromagnetic field profiles under the 500 kV power transmission lines at 1 m above ground.

Figure 5 presents the magnetic and electric fields induced around the insulators of the 220 kV line with a 100 kA striking current. For the 220 kV power line, the maximum induced magnetic and electric field values were approximately 59 kA/m

and 36 MV/m, respectively. For the 500 kV power line, the maximum induced magnetic and electric field values were approximately 57.3 kA/m and 34 MV/m. Table IV shows the induced electromagnetic field values for lightning striking in different phases and ground conductors for both 500 and 220 kV power transmission lines in front of the tower position and in front of the mid-span at 1 m above ground.
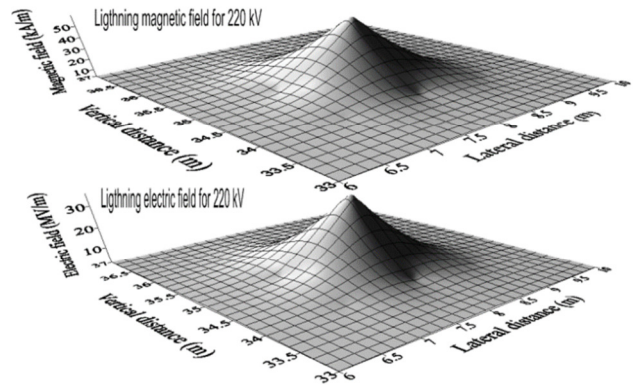

Fig. 5.   Lightning field profiles around the insulator of the 220 kV power line.

TABLE IV.   LIGHTNING-INDUCED ELECTROMAGNETIC FIELD VALUES FOR 500 AND 220 KV POWER LINES FOR DIFFERENT STRIKING POINTS

Lightning electromagnetic fields at ROW for 500 kV power line				
Striking point	In front of the tower		In front of the mid-span	
	(A/m)	(kV/m)	(A/m)	(kV/m)
Phase A	604.9	227.9	688.1	259.2
Phase B	463.6	174.7	486.2	183.2
Phase C	882.7	332.6	1222.2	460.5
G1	644.6	242.8	1006.1	379.1
G2	464.0	174.8	539.6	203.3
Lightning electromagnetic fields at ROW for 220 kV power line				
Striking point	In front of the tower		In front of the mid-span	
	(A/m)	(kV/m)	(A/m)	(kV/m)
Phase A1	634.4	239.03	676.7	254.9
Phase A2	1140.2	429.6	1557.8	586.9
Phase B1	532.97	200.83	575.52	216.85
Phase B2	828.6	312.2	1101.23	414.9
Phase C1	473.8	178.5	518.5	195.4
Phase C2	570.01	214.8	678.2	255.5
G. cond.	453.8	170.9	506.76	190.9

Figure 6 presents the induced current at different positions of the phases and the two ground conductors for the striking position of phase C of 500 kV. The maximum value of the striking current is -100 kA and tr/tt = 1/200 µs. The peak values of the current induced at different positions depend mainly on the relative distances between the striking point and the monitoring points. The maximum value of the induced current was approximately 23 kA on the ground conductor G1, while for Phase A, the maximum value of the induced current was approximately 20 kA. The results obtained were compared with [17] and found to be highly consistent.
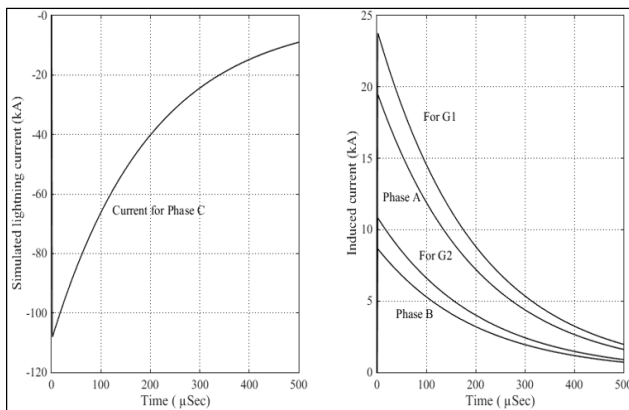
Fig. 6.   Lightning current and induced currents on different phases and ground conductors for 500 kV power transmission lines.

V.   CONCLUSIONS

The results obtained indicate that FDTD can be used to model and simulate lightning electromagnetic fields around 500 and 220 kV power transmission lines. Comparing the results obtained from the FDTD model and analytical solutions shows a small deviation, less than 2%. The simulation results showed that the lightning electromagnetic field at the selected points depends mainly on the relative position of the striking point. The results of lightning electromagnetic fields could be used for electromagnetic compatibility studies and insulation coordination, and in the early design stage of power transmission lines. Comparison of these results with previous studies and standards exhibited great convenience with a minor deviation. The lightning electromagnetic fields at the ROW of the two lines were evaluated at different positions to guide environmental studies. The maximum values of the lightning electromagnetic fields around the insulator were 57.4 kA/m and 35 MV/m. These values depend on the peak value of the striking lightning currents. The results of this study can be helpful to researchers in this field to withstand the exposure of electromagnetic fields around transmission lines.

REFERENCES

[1]   I. S. Grant, "A Simplified Method for Estimating Lightning Performance of Transmission Lines A Report Prepared by the Working Group on Lightning Performance of Transmission Lines," *IEEE Power Engineering Review*, vol. PER-5, no. 4, pp. 48–48, Apr. 1985, https://doi.org/10.1109/MPER.1985.5528828.

[2]   I. A. Metwally and F. H. Heidler, "Improvement of the lightning shielding performance of overhead transmission lines by passive shield wires," *IEEE Transactions on Electromagnetic Compatibility*, vol. 45, no. 2, pp. 378–392, Feb. 2003, https://doi.org/10.1109/TEMC.2003.811300.

[3]   "Protection against lightning - Part 3: Physical damage to structures and life hazard," International Electrotechnical Commission, Geneva, Switzerland, IEC 62305-3, Jan. 2006.

[4]   J. L. Bermudez *et al.*, "Far-field-current relationship based on the TL model for lightning return strokes to elevated strike objects," *IEEE Transactions on Electromagnetic Compatibility*, vol. 47, no. 1, pp. 146–159, Oct. 2005, https://doi.org/10.1109/TEMC.2004.842102.

[5]   Y. Baba and V. A. Rakov, "Lightning electromagnetic environment in the presence of a tall grounded strike object," *Journal of Geophysical Research: Atmospheres*, vol. 110, no. D9, 2005, https://doi.org/10.1029/2004JD005505.

[6]   D. Pavanello, "Electromagnetic radiation from lightning return strokes to tall structures," Ecole Polytechnique Federale de Lausanne, Switzerland, 2007.

[7]   H. B. Duc, T. P. Minh, T. P. Anh, and V. D. Quoc, "A Novel Approach for the Modeling of Electromagnetic Forces in Air-Gap Shunt Reactors," *Engineering, Technology & Applied Science Research*, vol. 12, no. 1, pp. 8223–8227, Feb. 2022, https://doi.org/10.48084/etasr.4692.

[8]   A. P. Anagha and K. Sunitha, "Influence of Field Spacer Geometry on the Performance of a High Voltage Coaxial Type Transmission Line with Solid Dielectric Spacer in Vacuum," *Engineering, Technology & Applied Science Research*, vol. 7, no. 3, pp. 1605–1610, Jun. 2017, https://doi.org/10.48084/etasr.1188.

[9]   K. Berger, "Parameters of lightning flashes," *Electra*, vol. 80, pp. 223–237, 1975.

[10]   R. B. Anderson, "Lightning parameters for engineering application," *ELECTRA*, vol. 69, pp. 65–102, 1980.

[11]   A. M. Hussein, M. Milewski, and W. Janischewskyj, "Correlating the Characteristics of the CN Tower Lightning Return-Stroke Current with Those of Its Generated Electromagnetic Pulse," *IEEE Transactions on Electromagnetic Compatibility*, vol. 50, no. 3, pp. 642–650, Dec. 2008, https://doi.org/10.1109/TEMC.2008.924398.

[12]   K. Yee, "Numerical solution of initial boundary value problems involving maxwell's equations in isotropic media," *IEEE Transactions on Antennas and Propagation*, vol. 14, no. 3, pp. 302–307, Feb. 1966, https://doi.org/10.1109/TAP.1966.1138693.

[13]   Y. Baba and V. A. Rakov, "Electromagnetic models of the lightning return stroke," *Journal of Geophysical Research: Atmospheres*, vol. 112, no. D4, 2007, https://doi.org/10.1029/2006JD007222.

[14]   Y. Baba and V. A. Rakov, "Applications of Electromagnetic Models of the Lightning Return Stroke," *IEEE Transactions on Power Delivery*, vol. 23, no. 2, pp. 800–811, Apr. 2008, https://doi.org/10.1109/TPWRD.2007.916169.

[15]   T. P. Minh *et al.*, "Finite Element Modeling of Shunt Reactors Used in High Voltage Power Systems," *Engineering, Technology & Applied Science Research*, vol. 11, no. 4, pp. 7411–7416, Aug. 2021, https://doi.org/10.48084/etasr.4271.

[16]   A. Mimouni, F. Delfino, R. Procopio, and F. Rachidi, "On the Computation of underground Electromagnetic Fields Generated by Lightning: A Comparison between Different Approaches," in *2007 IEEE Lausanne Power Tech*, Jul. 2007, pp. 772–777, https://doi.org/10.1109/PCT.2007.4538413.

[17]   H. Anis *et al.*, "Computation of Power Line Magnetic Fields - A Three Dimensional Approach," in *9th International Symposium on High Voltage Engineering (ISH)*, Graz, Austria, Aug. 1995.

[18]   D. Djalel and L. Hocine, "Study and characterization of the transient electromagnetic field radiated by lightning," in *4th International Conference on Power Engineering, Energy and Electrical Drives*, Istanbul, Turkey, Feb. 2013, pp. 511–516, https://doi.org/10.1109/PowerEng.2013.6635661.

[19]   R. Thottappillil, "Electromagnetic pulse environment of cloud-to-ground lightning for EMC studies," *IEEE Transactions on Electromagnetic Compatibility*, vol. 44, no. 1, pp. 203–213, Oct. 2002, https://doi.org/10.1109/15.990727.

[20]   "Protection of structures against lightning - Part I: General principles," International Electrotechnical Commission, Geneva, Switzerland, IEC 61024-1, 1998.

[21]   F. Rachidi, "Modeling Lightning Return Strokes to Tall Structures: A Review," *Journal of Lightning Research*, vol. 1, pp. 16–31, 2007.

[22]   A. Taflove, S. C. Hagness, and M. Piket-May, "Computational Electromagnetics: The Finite-Difference Time-Domain Method," in *The Electrical Engineering Handbook*, Elsevier Inc, 2005, pp. 629–670.

[23]   T. Rylander, P. Ingelström, and A. Bondeson, *Computational Electromagnetics*. New York, NY,USA: Springer, 2013.

[24]   G. Mur, "Absorbing Boundary Conditions for the Finite-Difference Approximation of the Time-Domain Electromagnetic-Field Equations," *IEEE Transactions on Electromagnetic Compatibility*, vol. EMC-23, no. 4, pp. 377–382, Aug. 1981, https://doi.org/10.1109/TEMC.1981.303970.